

Auroral electrojets during geomagnetic storms

Y. I. Feldstein

Institute of Terrestrial Magnetism, Ionosphere, and Radio Wave Propagation, Troitsk, Moscow Region

A. Grafe

GeoResearch Center, Potsdam, Germany

L. I. Gromova and V. A. Popov

Institute of Terrestrial Magnetism, Ionosphere, and Radio Wave Propagation, Troitsk, Moscow Region

Abstract. On the basis of digital magnetometers from the International monitor auroral geomagnetic effects (IMAGE) and European incoherent scatter (EISCAT) meridional chains in Scandinavia dynamics of the eastward and westward electrojets during the main phase of magnetic storms are considered. For the intense magnetic storm on May 10–11, 1992, with $Dst = -300$ nT, magnetograms of subauroral and midlatitudinal stations Leningrad, Borok, and Moscow were examined. It is found that the eastward electrojet center during the storm main phase shifts equatorward as $|Dst|$ increases. The electrojet center is located at the corrected geomagnetic latitude $\Phi \sim 59^\circ\text{--}60^\circ$ when $Dst \sim -100$ nT and at $\Phi \sim 54^\circ\text{--}55^\circ$ when $Dst \sim -300$ nT. Data from meridional chains of magnetometers support earlier results pertaining to the relationship between the westward electrojet center position and the ring current intensity for intervals between substorms. During substorms expansive phases the westward electrojet expands poleward covering auroral latitudes $\Phi \sim 65^\circ$. The electrojets location during the storm main phase and their dynamics in connection with substorms allow for interpretations of effects described in the literature: the AE indices saturation during the main phase of magnetic storms; approximately equal values of AU and AL indices during the storm initial phase and $AL \gg AU$ during the storm main phase.

Introduction

The auroral electrojet intensification is a characteristic feature of geomagnetic field disturbances [Chapman and Bartels, 1940]. The electrojets reach their maximum intensity at auroral latitudes and the auroral electrojet indices (AE , AU , AL) were introduced for description of the electrojets by Davis and Sugiura [1966]. Since then, they have been extensively used as measures of the auroral electrojet intensity and of magnetospheric activity during substorms and storms. The standard auroral indices are calculated on the basis of data from 12 magnetic observatories constituting a longitudinal chain over corrected geomagnetic latitudes between 63° and 70° [Allen, 1970; Allen et al., 1976; Kamei and Maeda, 1981].

The variations of the electrojet indices have limited accuracy for several reasons: (1) inhomogeneous distribution of the AE observatories versus the longitude;

(2) differences in the latitudes of the observatories; and (3) limited latitudinal coverage of the AE observatories locations.

Kamide and Akasofu [1983] and Akasofu et al. [1983] investigated the accuracy of the auroral electrojet indices. It was shown that during relatively quiet periods, standard AE stations are not able to monitor properly the activity of the auroral electrojets. The ratio $AE(12)/AE(71)$ (here $AE(12)$ is AE index determined using 12 auroral observatories and $AE(71)$ is the same index determined on the basis of data from 71 observatories) sharply decreases for $AE(12) < 400$ nT. It arises out of the poleward shift of the electrojet during quiet intervals that causes the standard observatories to escape from the zone directly influenced by the electrojets. The results of their investigation was based on data from six meridional chain stations for March 17, 18, and 19, 1978, encompassing both relatively quiet intervals and intervals with intense substorms.

Since the auroral oval expands equatorward and contracts poleward in association with the interplanetary magnetic field variations and substorms activity, one might expect a sharp decrease in $AE(12)$ during in-

Copyright 1997 by the American Geophysical Union.

Paper number 97JA00577.
0148-0227/97/97JA-00577\$09.00

tense disturbances as well. *Kamide and Akasofu* [1974] analysed the latitudinal dependence of the westward auroral electrojet profile across the Alaska meridian chain of observatories, finding that during substorms with intensity as high as ~ 1000 nT, the maximum deviation of the horizontal component from the quiet level is located at the auroral zone at $\Phi \sim 65^\circ$.

Akasofu [1981] studied the *Dst*-*AE* relationship for a few intense magnetic storms and found that at the moderate storm level *AE* and $|Dst|$ grow together in a practically linear manner. However, for more intense storms, he found that *AE* tends to saturate at a level of ~ 1000 nT. It was suggested that as a storm develops, the division of energy entering the magnetosphere between the ring current and the auroral ionosphere changes. At the beginning of a storm, when $|Dst|$ is small, there is proportionality between the energy injection to the ring current and the auroral ionosphere. During the main phase of intense magnetic storms, most of the energy goes to the ring current. Similar *AE*-*Dst* relationship as a function of the storm intensity is presented by *Gonzalez et al.* [1994].

Weimer et al. [1990] studied the *AE*- B_z relationship, where B_z is north-south component of the interplanetary magnetic field. Saturation of *AE* takes place when B_z is southward and intense. Such B_z values are accompanied, as a rule, by the intense ring current generation.

Akasofu [1981] and *Weimer et al.* [1990] considered various causes of the saturation effect, including among others the shift of the auroral electrojets toward the equator during the main phase of magnetic storms. However, this possibility was rejected in favor of either energy redistribution or the nonlinear response of the magnetosphere-ionosphere system to the magnetospheric disturbances. According to *Weimer et al.* [1990], the westward electrojet center never shifts equatorward of Sitka ($\Phi = 60^\circ$).

Sumaruk et al. [1989], *Feldstein* [1992], and *Feldstein et al.* [1994] have suggested that the apparent saturation or even decrease of *AE* during the main phase of intense storms can be due to the auroral electrojets moving considerably lower latitudes so that the *AE* stations do not correctly monitor the substorm evolution. For more precise calculations of the *AE* indices during magnetic storms, it is necessary to use data from magnetic observatories at subauroral latitudes where the auroral electrojets shift during magnetic storms. Below, investigation of the eastward and westward electrojets dynamics is continued using data from the digital magnetic stations meridional chain along the Scandinavian peninsula (EISCAT and later IMAGE) supplemented by analogue magnetograms of Leningrad, Borok, and Moscow during an intense magnetic storm. These Russian stations are located near the same magnetic meridian. The aim of this paper is documentation of the electrojet dynamics during magnetic storms. The number of stations equatorward of the auroral oval along this meridian is unique at the present time. Table 1 presents the coordinates of all stations used in the analysis.

Table 1. Coordinates of the Magnetic Observatories

Observatory	Code	Geographic Coordinates		Geomagnetic Coordinates	
		Lat	Long	Lat	Long
Soroya	SOR	70.54N	22.22E	67.21	106.91
Keva	KEV	69.76	27.01	66.15	109.93
Masi	MAS	69.46	23.70	66.04	107.10
Kilpisjarvi	KIL	69.02	20.79	65.80	104.45
Muonio	MUO	68.02	23.53	64.60	105.82
Pello	PEL	66.90	24.08	63.43	105.52
Oulujarvi	OUL	64.52	27.23	60.86	106.60
Hankasalmi	HAN	62.30	26.65	58.60	105.02
Nurmijarvi	NUR	60.50	24.65	56.79	102.51
Leningrad	LNN	59.95	30.70	55.79	107.78
Borok	BOX	58.02	39.00	53.60	114.78
Moscow	MOS	55.50	37.30	50.99	111.97

Auroral Electrojet Dynamics During a Moderate Magnetic Storm on April 1993

Figure 1 presents variations of the northern (X) component of the geomagnetic field along the IMAGE chain during the moderate magnetic storm with an initial phase onset that occurred between 0900 and 1000 UT on April 4, 1993. The storm main phase, connected with sharp decreases of the geomagnetic field horizontal component at low-latitude observatories, falls within the interval 1430 UT on April 4 to 0700 UT on April 5, 1993. Then, a slow recovery to the quiet level begins, lasting for several days. The IMAGE chain during the storm main phase was initially located in the longitudinal sector of the eastward electrojet (evening hours) and then in the longitudinal sector of the westward electrojet (night and early morning hours). Vertical dotted lines mark latitudinal cross sections. The first two cross sections (N1 and N2) characterize the eastward electrojet at the auroral zone latitudes. The cross sections N3 and N4 describe the geomagnetic field distribution relative to the Harang discontinuity, where at latitudes equatorward of the discontinuity $\Delta X > 0$ and poleward of the discontinuity $\Delta X < 0$. Data in Figure 1 show a clear shift of the eastward directed current ($\Delta X > 0$) to the lower latitudes as the magnetic storm main phase develops in the interval 1400-1800 UT on April 4, 1993.

Besides temporal UT effects in the eastward electrojet locations caused by the magnetospheric ring current and the tail current development, LT effects are also possible from the asymmetry of the inner magnetosphere versus the local time. Therefore the latitudinal cross section N9 on April 5, 1993, was selected during the recovery phase at the same UT (1430 UT) as the cross section N1 during the storm initial phase. This difference between two latitudinal cross section, as far as location of the eastward electrojet is concerned, should be caused by variations in the intensity of the ring current and the tail current during the storm initial and

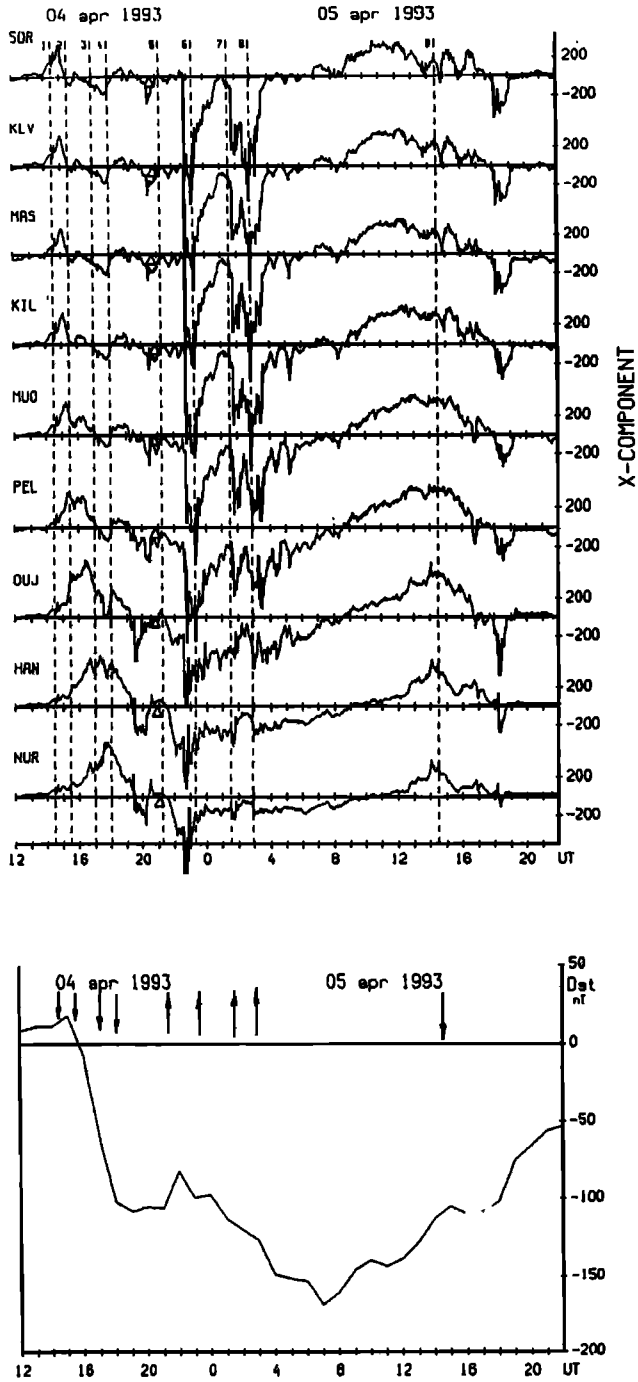


Figure 1. Variations of the X component magnetic field along the IMAGE chain during storm main phase on April 4-5, 1993 (at the top). The intensity was measured relative to the quiet level at 0900-1100 UT on April 4. Dotted lines (vertical) correspond to nine universal times with latitudinal cross sections of the ΔX and ΔZ components presented further in the text. The Dst variation of the magnetic field for the same storm is shown at the bottom. Arrows directed downwards mark universal times of latitudinal cross sections through the eastward electrojet, and arrows directed upward mark cross section through the westward electrojet. The location of the magnetic midnight in each station is marked by triangle.

recovery phases. The existence of such LT variations in the eastward electrojet location is clearly seen for 1000-1600 UT on April 5.

Latitudinal cross sections N5 - N8 were specially selected to characterize the westward electrojet dynamics during the transition from the relatively quiet interval prior to the substorm onset to the maximum of the substorm expansion phase. During the period of the extremely low Dst values from 0600 to 0900 UT on April 5 the magnetic field variations along the magnetometer chain are near the quiet level. Such attenuations of the magnetic disturbances along the IMAGE chain are most likely due to the shift of the chain meridian to the day sector where the westward electrojet is located poleward of normal auroral zone latitudes [Akasofu, 1968].

Latitudinal cross sections of ΔX and ΔZ through the eastward electrojet at consecutive UT times are presented in Figure 2. Arrows mark the location of the center of the eastward electrojet. The equatorward shift of the eastward electrojet center from $\sim 67^\circ$ at 1430 UT to $\sim 57^\circ$ at 1800 UT is distinctly seen during the storm main phase. During the recovery phase, the electrojet center begins to return to the initial position, but its location at 1430 UT on April 5 is still substantially more equatorward than its location at the onset time of the storm initial phase (1430 UT on April 4). At 1700-1800 UT, $\Delta X < 0$ in the poleward part of the latitudinal cross section. This is due to the appearance at these latitudes in the evening sector of the westward directed currents. This corresponds to an increase in the size of the dawn westward ionospheric current cell as described by Fukushima [1953]. However, the eastward electrojet does not disappear in the evening sector as disturbances increase. Instead it shifts to subauroral latitudes with Dst intensification. The observed shift of the eastward electrojet to subauroral latitudes during storm main phase leads to a substantial underestimation of the AU (AE) indices determined on the basis of auroral zone latitude observatories only.

The character of latitudinal cross sections through the westward electrojet, presented in Figure 3, and the eastward electrojet are substantially different. During relatively quiet intervals between substorms, such as 2116 UT on April 4, 1993, and 0132 UT on April 5, 1993 the electrojet center was located at $\Phi \sim 61^\circ$ near midnight-early morning MLT, i.e., in the equatorward part of the auroral zone. At the substorm maximums which occur at 2320 UT on April 4 and 0255 UT on April 5, the electrojet center does not shift equatorward but the electrojet sharply widens poleward. The maximum ΔX field decrease occurs at $\Phi \sim 64^\circ-65^\circ$, i.e., at the central latitudes of the auroral zone. It is at these latitudes that observatories used for the AE indices calculation are placed. Thus, during magnetic storms intervals, the AL indices are correctly determined during the substorm expansive phase maximum and are significantly underestimated during the intervals between substorms.

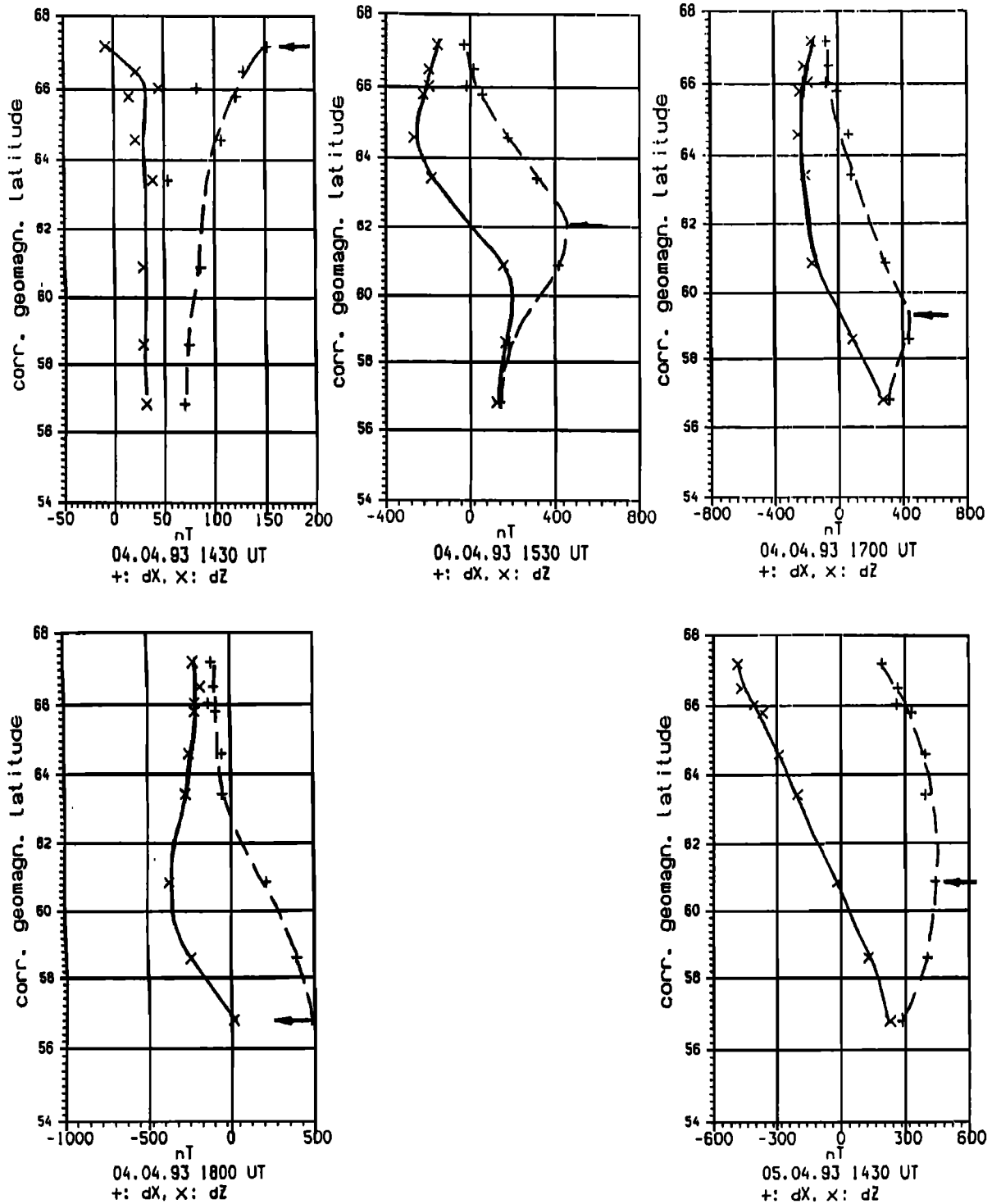


Figure 2. The latitudinal cross sections ΔX (dotted line) and ΔZ (solid line) through the eastward electrojet on April 4, 1993, at 1430, 1530, 1700, and 1800 UT, April 5 at 1430 UT. Arrows mark the latitudes of the eastward electrojet center.

Auroral Electrojet Dynamics in an Interval of Intense Magnetic Storm Activity on May 10-11, 1992

All stations of the IMAGE chain began to operate in Finland in 1993. The chain recorded several moderate magnetic storms with extremum values of Dst

< -150 nT. The auroral electrojet dynamics during the course of one such storms were presented in the previous section. The EISCAT meridional chain, the predecessor of IMAGE, recorded more intense magnetic storms. Figure 4 shows variations of the X component during the main phase and beginning of the recovery phase of the intense magnetic storm on May 10-11, 1992. The

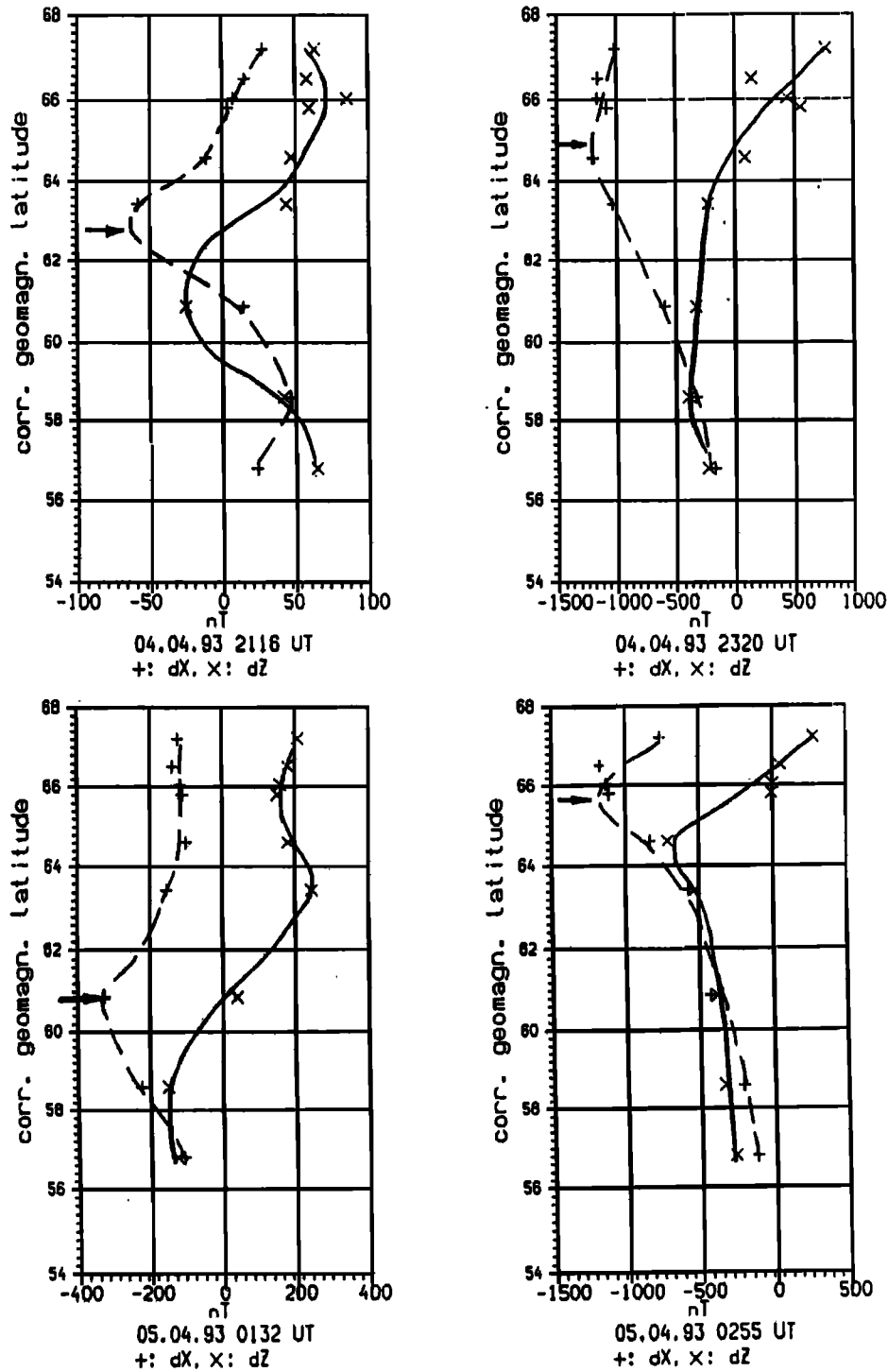


Figure 3. The latitudinal cross sections through the westward electrojet. At the left side, cross sections are presented at the universal times of quiet intervals between substorms (April 4, 1993 at 2116 UT and April 5 at 0132 UT), at the right side - at the universal times of substorms maxima (April 4, 1993 at 2320 UT and April 5 at 0255 UT). Arrows mark the latitudes of the westward electrojet center.

EISCAT chain did not include the field variations at Oulujarvi and Hankeisalmi, which are very important when studying the electrojet dynamics during moderate magnetic storms. For intense magnetic storms with $Dst < -200$ nT it appeared necessary to use observations from Russian magnetic stations located approxi-

mately along the EISCAT meridian up to $\Phi \sim 51^\circ$. The eastward electrojet shifts equatorward of the EISCAT chain during intense magnetic storms.

For the May 10, 1992, storm intense $\Delta X > 0$ at the subauroral stations appear immediately after the local geomagnetic noon and reach a maximum of 1154 nT

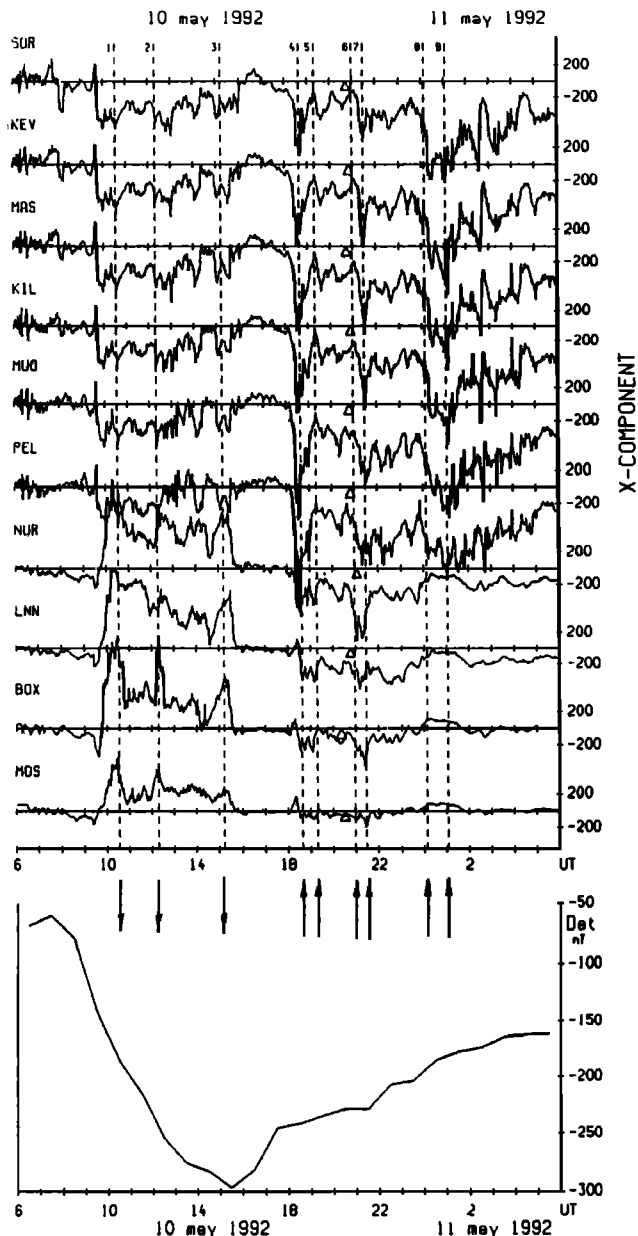


Figure 4. Variation of the magnetic field component along the EISCAT chain during the main phase of the storm on May 10-11, 1992 (at the top). The intensity was measured relative to the level at 0600-0800 UT on May 10, 1992. Variations of the X components are added for Leningrad, Borok, and Moscow. The Dst variation of the magnetic field for the same storm is presented (at the bottom). Notations are similar to Figure 1.

at 1030 UT. In the auroral zone, where ΔX is usually positive in the evening hours, the westward currents were recorded during this time. Such currents flow in the auroral zone during the whole storm main phase. Hence, if only the region of auroral latitudes is considered, the impression can be created that the eastward electrojet disappear during the course of intensive magnetic storms. Latitudinal cross sections ΔX and ΔZ , when subauroral and midlatitude observatories record-

ed the eastward electrojet, are presented in Figure 5. The eastward electrojet center location is $\Phi \sim 54^\circ$ - 55° . The current direction changes at $\Phi \sim 61^\circ$ (Harang discontinuity). The appearance of this discontinuity at such low latitudes and early MLT (~ 13) occurs only during intervals of intense magnetic storms.

Figure 6 shows latitudinal cross sections ΔX and ΔZ for times when the westward current was located above all the chain stations. The absence of Oulujarvi and Hankasalmi data prohibits the reasonably precise localization of the westward electrojet center. However, the field variations clearly show that at the times of maxima substorm intensity the electrojet center is located at higher latitudes than during the intervals between substorms or in the beginning of the expansion phase of substorms at auroral latitudes.

Discussion

During the storm main phase it is necessary to take into account data from subauroral observatories for the AE indices calculation. The usage of corrected AE indices has previously shown [Feldstein *et al.*, 1994], that (1) during the storm main phase energy fluxes in the ring current and those of the auroral ionosphere increase simultaneously and (2) during the storm main phase there exists close relationship between the geoeffective solar wind parameters and energy flux entering in the magnetosphere.

The eastward electrojet dynamics during geomagnetic storms was investigated by Kamide and Fukushima [1972], Grafe [1983], and other. As a rule, the electrojet center shifts equatorward during a substorm but practically always lies within the auroral zone at $\Phi \sim 63^\circ$ - 65° . The center shift during the magnetic storm of April 4, 1993, is shown in Figure 2. For the determination of the eastward electrojet center within 10 min intervals, a model of a homogeneous current layer at 120 km altitude above the Earth's surface [Grafe *et al.*, 1987] was used. The results for every 10-min interval are depicted in Figure 7 by a solid line. The electrojet center gradually shifts equatorward up to $\Phi \sim 57^\circ$ at 1800 UT during the storm main phase and then, when Dst stabilizes at the level of -100 nT for a short while, returns to $\Phi \sim 60^\circ$. At the beginning of the recovery phase, when $Dst \sim -100$ nT, the electrojet center is located at $\Phi \sim 60^\circ$. The latitude of 60° should thus be the location of the eastward electrojet center for the stable Dst level with intensity ~ -100 nT. The joint influences of the ring current and substorms shifts the eastward electrojet center somewhat equatorward, which is observed at 1800 UT.

A more sophisticated model of the ionospheric current distribution based on the magnetic field measurements along the meridian chain was used by Popov and Feldstein [1996]. The latitude interval above the magnetometer chain was divided into 50 infinitely thin bands layer at 115 km altitude. Current bands are assumed to be infinitely long, and the current density j in every band is homogeneous and determined by Biot-Savart's

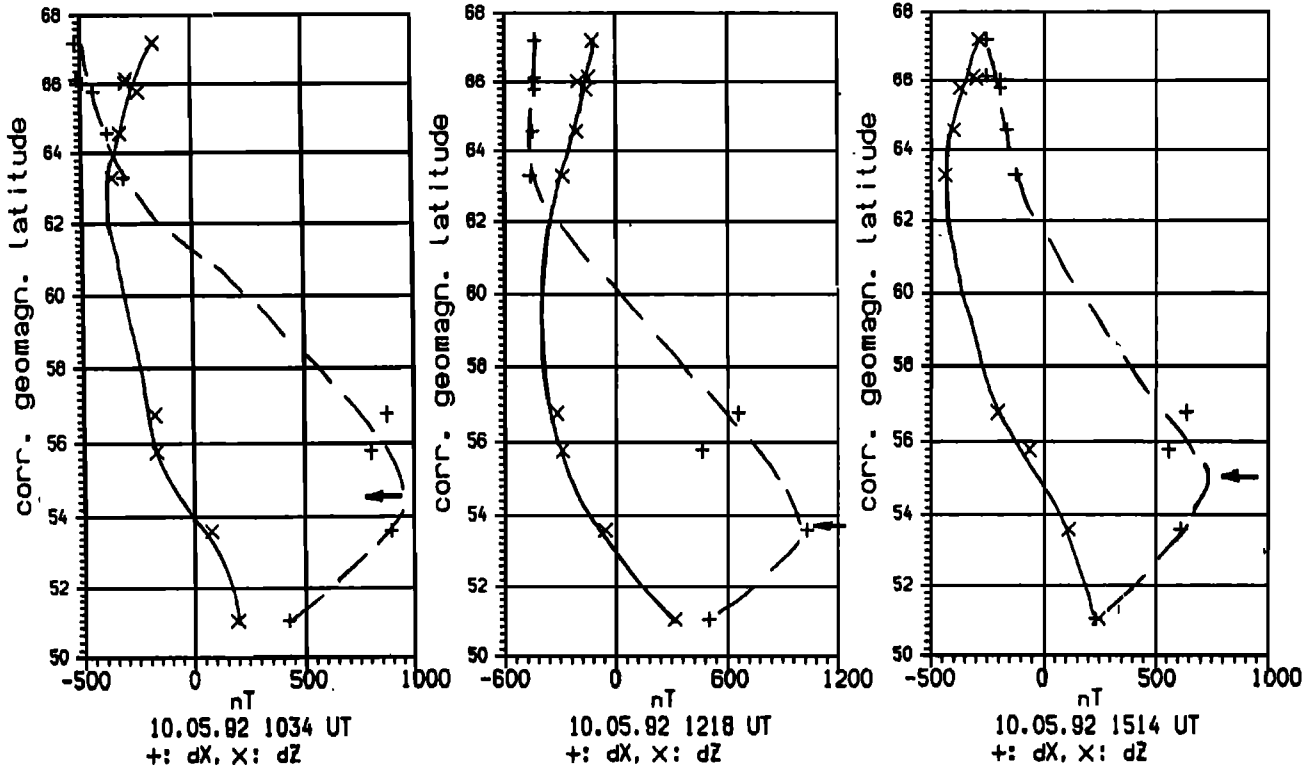


Figure 5. The latitudinal cross section X (dotted line) and Z (solid line) through the eastward electrojet on May 10, 1992, at 1034, 1218, and 1514 UT. Notations are similar to Figure 2.

law. To obtain a detailed structure of the meridian cross section of j , i.e., current values at 50 points, the inverse problem is solved by the regularization method [Tikhonov and Arsenin, 1974]. The model allows the separation of the observed ground magnetic field variations into internal and external sources. Figure 8 presents the latitudinal distribution of external (ionospheric) source currents calculated using the method developed by Popov and Feldstein [1996]. The eastward currents are spread over a large range of latitude. Arrows mark the latitudes of the current maximum, which shifts equatorward as the magnitude of Dst increases. The latitudinal profiles allow the integral current values to be calculated. For example, integral values of the eastward current in the Figure 8 cross sections, are 61.5×10^3 A at 1430 UT, 417.8×10^3 A at 1530 UT, 476×10^3 A at 1700 UT, 597×10^3 A at 1800 UT on April 4 and 525×10^3 A at 1430 UT on April 5. The comparison of the current integral values and the current maximum values along the latitudinal cross sections shows that they change asynchronously. The integral current values take into account not only the intensity, but the electrojet width, and, therefore it is more precise characteristic of disturbance level, according to Kamide and Akasofu [1974], than AU or AL indices.

Figure 9 shows the location of the westward electrojet center during the main phase of the magnetic storm in the near-midnight to early dawn MLT sector for intervals between substorms versus Dst [Feldstein,

1992]. The numerals near the circles are UT hours for the March 23-24, 1969, strong magnetic storm. The straight line has been obtained by the least squared method. The electrojet moves to the lower latitudes as DR increases and its position is described by the relationship

$$\Phi = 65.2^\circ + 0.035DR \quad (1)$$

in the $0 > DR > -250$ nT interval, where DR is in nanoteslas. Crosses in Figure 9 correspond to the westward electrojet center in the intervals between substorms for the April 4-5, 1993 and May 10-11, 1992, magnetic storms. Good quantitative agreement of data for all three magnetic storms is clearly seen. Thus the data of the IMAGE and the EISCAT meridian chains of magnetometers support the earlier obtained relationship between the westward electrojet center position and the DR or Dst intensity.

During the storm main phase the center of the westward auroral electrojet shifts equatorward to $\Phi \sim 58^\circ$ when $Dst \sim -200$ nT and $\Phi \sim 54^\circ$ when $Dst \sim -300$ nT. Assuming quasi-dipole character of the magnetic field lines in the inner magnetosphere, it means the location of the electrojet at L shells of ~ 3.6 and ~ 2.9 , respectively. Lyons [1996] suggest that the processes, connected with the electrojet formation deeply in the inner magnetosphere, can be the cause of energetic ion fluxes which form the low energy part of the ion spectra in the inner part of the ring current. These ions are mainly oxygen from the upper atmosphere which

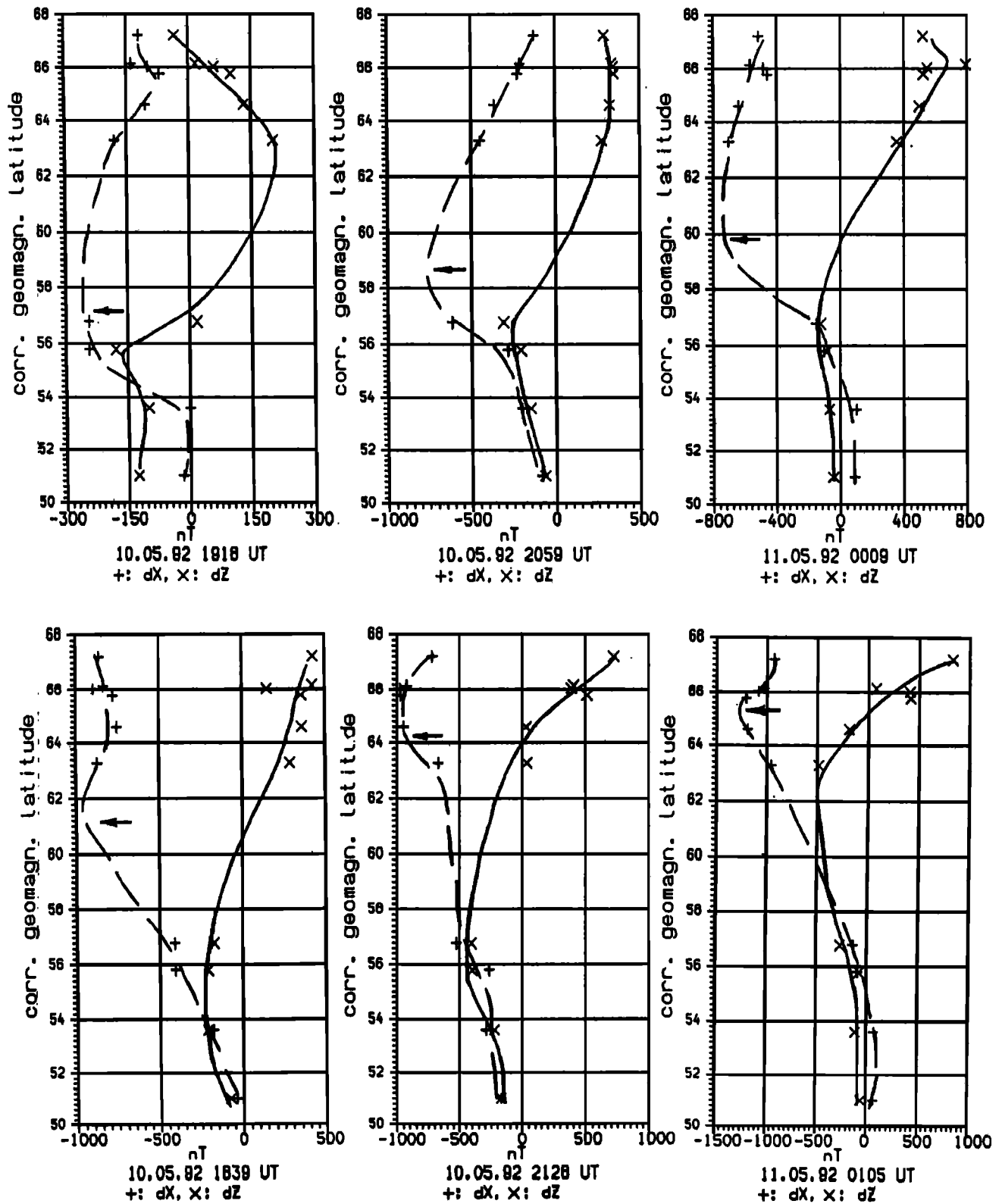


Figure 6. The latitudinal cross sections through the westward electrojet during intervals between substorms or in the beginning of a substorm expansion phase in auroral latitudes on May 10, 1992, at 1918, 2059 UT and on May 11 at 0009 UT and at substorms maxima on May 10 at 1839, 2128 UT and May 11 at 0105 UT. Notations are similar to Figure 3.

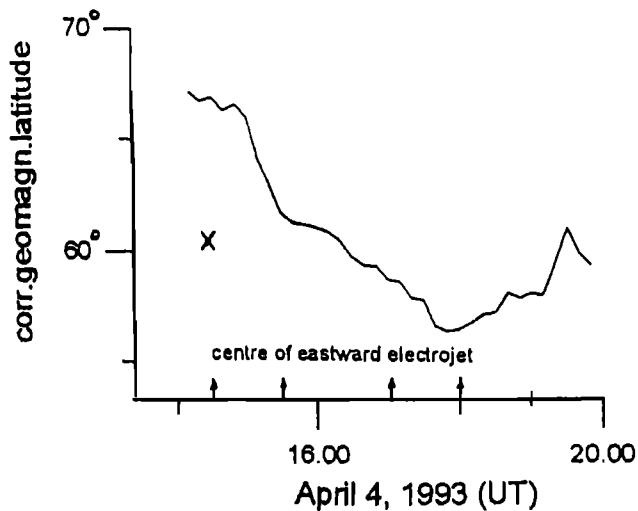


Figure 7. The eastward electrojet center shifts for the storm main phase on April 4, 1993 (solid line). The cross marks the center position at 1430 UT on April 5. Arrows mark universal times of the latitudinal cross sections in Figure 2.

can be accelerated up to ~ 10 keV energy directly from the ionospheric heights. However, the bulk ion population in the ring current has energy in the 50-100 keV interval. Apparently, ions of such energies are accelerated from the ionosphere at higher latitudes during intense substorms, when the westward electrojet widens poleward and its maximum intensity at the substorm maximum occur at the central latitudes of the auroral zone. From those latitudes ions of ionospheric origin enter the plasma sheet and then move earthward (large-scale magnetospheric convection). It is possible that the ionospheric ion flux toward the plasma sheet at the substorm maximum is substantially larger than that toward the inner magnetosphere during intervals between substorms. When convecting earthward, allowing for the first adiabatic invariant conservation, ions acquire additional energy and constitute the main population of the ring current with energies of several dozens keV.

The electrojet location during the storm main phase and their dynamics in connection with substorms allow to interpret some effects described in the literature. Among them is the *AE* saturation effect described by Weimer *et al.* [1990]. It occurred when B_z is southward with a large magnitude, i.e., during storm main phase. It was assumed that the *AE* saturation is the result of the nonlinear nature of the magnetosphere-ionosphere coupling [Kan *et al.*, 1988]. On the basis of electrojet dynamics discussed above for the storm main phase, the following interpretation can be offered for the *AE* saturation effect for *AE* minimum values and its absence for *AE* maximum values. For small *AE* values, i.e., during intervals between substorms, both the eastward and westward electrojets are located equatorward of the chain of observatories for intervals of large southward B_z component of the interplanetary

magnetic field (IMF). In this situation a change in the IMF B_z magnitude does not influence the *AE* intensity, i.e., we have the saturation effect in the *AE* indices. The maximum of the *AE* indices is related to the sharp poleward widens of the westward electrojet. The chain of the *AE* observatories begin to record the electrojet with the maximum intensity in close connection with the magnitude of the IMF southward component, i.e., the saturation effect of the *AE* indices is absent.

Kamide [1979] discovered an interesting peculiarity in the behavior of the *AU* and *AL* indices during magnetic storms, namely, $AU = AL$ during the initial phase and $AU \ll AL$ during the main phase. This peculiarity of *AU* (*AL*) indices is a consequence of the electrojets dynamics in the course of a magnetic storm. At the initial phase, when the ring current is weak, the electrojet centers are located at *AE* observatories latitudes and, therefore, $AU = AL$. During the main phase the electrojets centers shift equatorward of the *AE* observatories latitudes, though the westward electrojet simultaneously widens poleward to the *AE* observatories latitudes. Such dynamics of the electrojets explains the peculiarity of *AU* (*AL*) indices behavior described by Kamide [1979].

The above presented analysis of the magnetic field variations during magnetic storms intervals shows that the eastward electrojet does not disappear when an intensive magnetic disturbance develops (this conclusion is valid for other storms as well). For the magnetic storm on May 10, 1992, the eastward electrojet, when $Dst \sim -300$ nT at 1500-1600 UT, was observed at subauroral and midlatitudinal stations Nurmijarvi, Leningrad, Borok, and Moscow, where the variations $\Delta X > 0$ reached ~ 1100 nT for Borok. The positive values of ΔX at these observatories existed for a long interval during the storm main phase, when intense *Dst* was accompanied by very intense eastward electrojet. It is quite possible, that conclusion on the existence of cases where there is no eastward electrojet anywhere during the main phase when the westward electrojet is very intense [Kamide *et al.*, 1976; Kamide, 1979] requires additional more careful substantiation. At any rate data from the meridian chains IMAGE and EISCAT shows that the eastward electrojet exists in the evening sector in every magnetic storm. The electrojet shifts equatorward of auroral zone latitudes occupying more and more early hours with increase of the *Dst* intensity.

The equatorward shift of the electrojet during magnetic storms should exist not only along the meridian of EISCAT-IMAGE magnetic observatories chains. Therefore, the inference of Weimer *et al.* [1990, p.18,984] that "by examining magnetic records from College ($\Phi = 65^\circ$) and Sitka ($\Phi = 60^\circ$) during the International Geophysical Year (one of the most disturbed periods over recorded in the century), we found that the *Z* component from Sitka almost always shows negative changes, indicating that the westward electrojet was located poleward of Sitka," requires on additional consideration using data from Sitka.

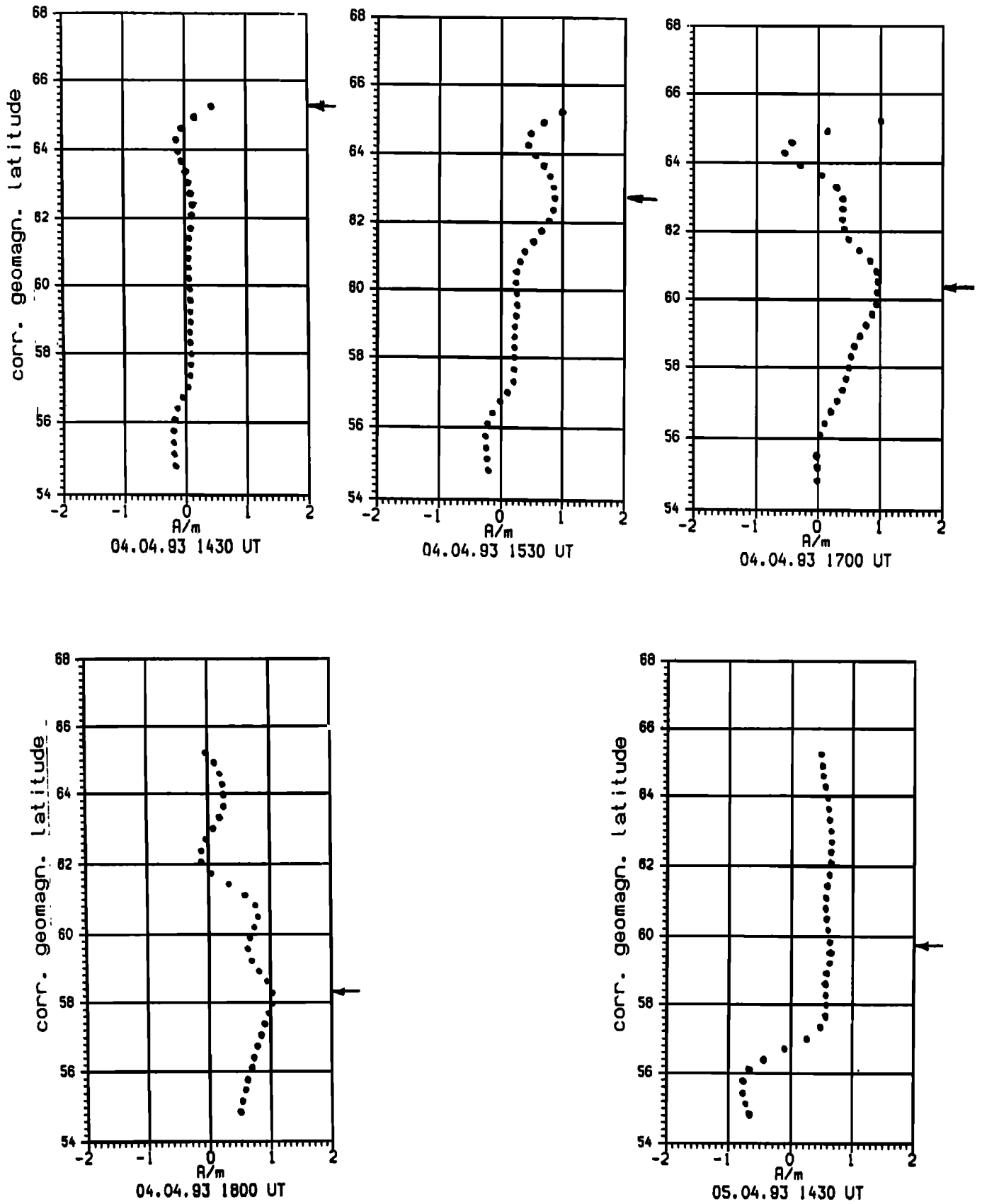


Figure 8. The latitudinal cross section of the current density j through the eastward electrojet from the external sources [Popov and Feldstein, 1996] for the magnetic storm on April 4-5, 1993. Arrows mark the current maximum position.

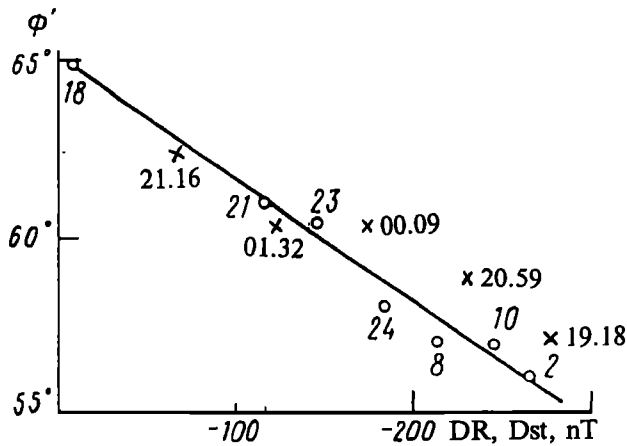


Figure 9. The position of the westward electrojet centers in the near-midnight-early dawn MLT sector as the function of DR or Dst intensity. The numerals at the circles and crosses are UT. The straight line has been obtained by the least-squares method.

Proper disturbance for such a consideration is the storm with main phase on September 29, 1978. The maximum values of $Dst \sim 250$ nT fall on ~ 1200 UT, i.e., near midnight hours for Sitka, when the intense westward electrojet is expected at the station meridian. Figure 10 presents for the period between September 28 and September 30 of 1978, the interplanetary medium parameters variations, the AE and Dst indices, and hourly mean values of horizontal (ΔH) and vertical (ΔZ) components of the magnetic field for Sitka. On September 28, 1978, the substorm with the AE intensity up to 1000 nT is characterized by the westward current with center poleward of Sitka ($\Delta H < 0$ and $\Delta Z < 0$). On September 29 during the storm main phase, the westward electrojet center ($\Delta H < 0$) was located initially poleward of Sitka ($\Delta Z < 0$) and then, as Dst variation intensifies, the electrojet center shifted to the zenith ($\Delta Z \sim 0$) and then farther equatorward ($\Delta Z > 0$) of station. Thus the data presented in Figure 10 indicate that intense westward electrojet is located

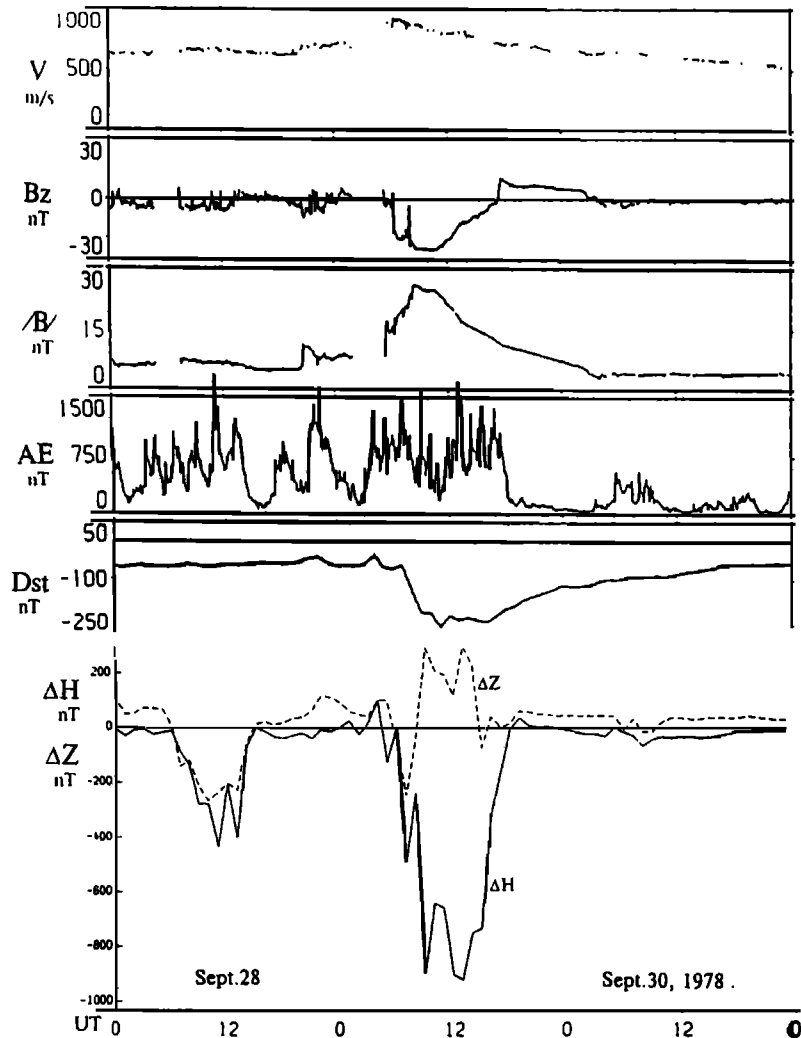


Figure 10. Variations of the solar wind speed, the B_z and $|B|$ of the IMF, indices AE and Dst , and Sitka's variations of the ΔH and ΔZ components (as deviations from quiet day field values) for the storm on September 28-30, 1978.

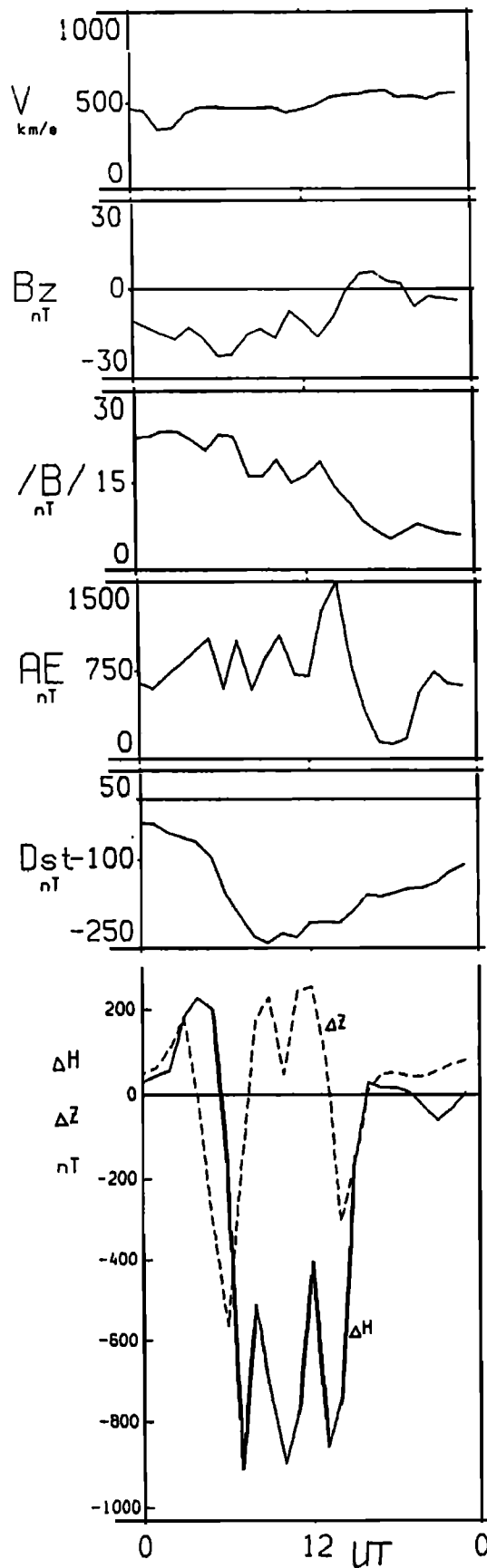


Figure 11. Data similar to presented in Figure 10, but for the storm on August 28, 1978.

poleward of Sitka ($\Phi = 60^\circ$) near midnight before the main phase of the intense magnetic storm but shifts equatorward of the station during the main phase.

The storm on September 29, 1978, is not unique. A similar situation was observed for the storm on August 28, 1978, as well. For this storm data on the interplanetary medium parameters, the geomagnetic activity indices and hourly mean values of the magnetic field variations for Sitka are shown in Figure 11. The westward electrojet center shifts to the station zenith as Dst develops and then moves equatorward of the station ($\Delta H < 0$, $\Delta Z > 0$).

Thus, during the main phase of magnetic storms ($Dst < -250$ nT) the one hour averaged westward electrojet is located equatorward of Sitka. Hence, near the Alaska meridian the westward electrojet center averaged for 1 hour is located equatorward of $\Phi = 60^\circ$ during the main phase of intense magnetic storms as well as over EISCAT-IMAGE.

Acknowledgments. We are grateful to EISCAT magnetometer and IMAGE teams for possibility to use magnetic observatories chain data. This research was supported by the Russian Foundation of Basic Research, grants 96-05-66279 and 96-05-65067, INTAS-RFBR-95-0932.

The Editor thanks S.-I. Akasofu and R. Nakamura for their assistance in evaluating this paper.

References

- Akasofu, S.-I., *Polar and magnetospheric substorms*, D. Reidel, Norwell, Mass., 1968.
- Akasofu, S.-I., Relationships between the AE and Dst indices during geomagnetic storms, *J. Geophys. Res.*, **86**, 4820-4822, 1981.
- Akasofu, S.-I., B. H. Ahn, Y. Kamide, and J. H. Allen, A note on the accuracy of the auroral electrojet indices, *J. Geophys. Res.*, **88**, 5769-5772, 1983.
- Allen, J. H., Auroral electrojet magnetic activity indices (AE) for 1970, *Rep. UAG-22*, World Data Cent. A Solar Terr. Phys., Natl. Oceanic and Atmos. Admin., Boulder, Colo., 1970.
- Allen, J. H., C. C. Abston, and L. D. Morris, Auroral electrojet magnetic activity indices AE (11) for 1973, *Rep. UAG-47*, World Data Cent. A Solar Terr. Phys., Natl. Oceanic and Atmos. Admin., Boulder, Colo., 1976.
- Chapman, S. C., and J. Bartels, *Geomagnetism*, Clarendon, Oxford, 1940.
- Davis, T. N., and M. Sugiura, Auroral electrojet activity index AE and its universal time variation, *J. Geophys. Res.*, **71**, 785-803, 1966.
- Feldstein, Y. I., Modelling of the magnetic field of magnetospheric ring current as a function of interplanetary medium, *Space Sci. Rev.*, **59**, 83-165, 1992.
- Feldstein, Y. I., A. E. Levitin, S. A. Golyshev, L. A. Dremuhina, U. B. Veshchezerova, T. E. Valchuk, and A. Grafe, Ring current and auroral electrojets in connection with interplanetary medium parameters during magnetic storm, *Ann. Geophys.*, **12**, 602-611, 1994.
- Fukushima, N., Polar magnetic storms and geomagnetic bays, *J. Fac. Sci. Tokyo Univ.*, **8**, 293-412, 1953.
- Gonzalez, W. D., J. A. Joselyn, Y. Kamide, H. W. Kroehl, G. Rostoker, and B. T. Tsurutani, What is a geomagnetic storm? *J. Geophys. Res.*, **99**, 5771-5792, 1994.
- Grafe, A., Electrojet boundaries and electron injection boundaries, *J. Geomagn. Geoelectr.*, **35**, 1-15, 1983.

- Grafe, A., R. J. Pellinen, W. Baumjohann, and M. Vallinkoski, Development of the auroral electrojets on 16 March 1978: An event study, *Geophysica*, **83**, 113-141, 1987.
- Kamei, T., and H. Maeda, Auroral electrojet indices (*AE*) for January-June, 1978, *Data Book 3*, Fac. Sci., Kyoto Univ., Kyoto, Japan, 1981.
- Kamide, Y., Relation between substorms and storms, in *Dynamics of the magnetosphere*, edited by S.-I. Akasofu, pp. 425-443, D. Reidel, Norwell, Mass., 1979.
- Kamide, Y., and S.-I. Akasofu, Latitudinal cross section of the auroral electrojet and its relation to the interplanetary magnetic field polarity, *J. Geophys. Res.*, **79**, 3755-3771, 1974.
- Kamide, Y., and S.-I. Akasofu, Notes on the auroral electrojet indices, *Rev. Geophys.*, **21**, 1647-1656, 1983.
- Kamide, Y., and N. Fukushima, Positive geomagnetic bays in evening high latitudes and their possible connection with partial ring current, *Rep. Ionos. Space Res. Jpn.*, **26**, 79-101, 1972.
- Kamide, Y., H. W. Kroehl, M. Kanamitsu, J. H. Allen, and S.-I. Akasofu, Equivalent ionospheric current representations by a new method, illustrated for 8 - 9 November 1969 magnetic disturbances, *Rep. UAG-55*, pp. 1 - 11, World Data Cent. A Solar Terr. Phys., Natl. Oceanic and Atmos. Admin., Boulder, Colo., 1976.
- Kan, J. R., L. Zhu, and S.-I. Akasofu, A theory of substorm: onset and subsidence, *J. Geophys. Res.*, **93**, 5624-5640, 1988.
- Lyons, L. R., Round-table discussion, paper presented at Chapman Conference on Magnetic Storm, AGU, Pasadena, Calif., Feb. 12-16, 1996.
- Popov, V. A., and Y. I. Feldstein, About a new interpretation of "Harang discontinuity", *Geomagn. Aeron.*, **36**, (1), 43-51, 1996.
- Sumaruk, P. V., Y. I. Feldstein, and B. A. Belov, The dynamics of magnetospheric activity during an intense magnetic storm, *Geomagn. Aeron.*, **29**, 110-115, 1989.
- Tikhonov, A. N., and V. Y. Arsenin, *Methods of noncorrect problems solution*, Moscow, Nauka, 1974.
- Weimer, D. R., L. A. Reinleitner, J. R. Kan, L. Zhu, and S.-I. Akasofu, Saturation of the auroral electrojet current and the polar cap potential, *J. Geophys. Res.*, **95**, 18981-18987, 1990.

Y. I. Feldstein, L.I.Gromova, and V. A. Popov, IZMIRAN, 142092 Troitsk, Moscow Region, Russia

A. Grafe, GeoResearch Center, D-14482 Potsdam, Germany

(Received April 26, 1996; revised October 21, 1996; accepted February 17, 1997.)